ChemElectroChem

Review
doi.org/10.1002/celc.202300802

Chemistry Europe
European Chemical Societies Publishing

www.chemelectrochem.org

Advancements in Addressing Microcrack Formation in Ni–Rich Layered Oxide Cathodes for Lithium–Ion Batteries

Tianmei Xu,[a] Jingjing Wu,[a] Juan Ding,*[a] Yingde Huang,*[c] Yudai Huang,[a] and Wengao Zhao*[b]

Nickel–rich layered oxides of $LiNi_{1-x-y}Co_xMn(Al)_yO_2$ (where 1–x–y > 0.6) are considered promising cathode active materials for lithium-ion batteries (LIBs) due to their high reversible capacity and energy density. However, the widespread application of NCM(A) is limited by microstructural degradation caused by the anisotropic shrinkage and expansion of primary particles during the H2→H3 phase transition. In this mini–review, we comprehensively discuss the formation of microcracks, subsequent material degradation, and related alleviation strategies in nickel–rich layered NCM(A). Firstly, theories on microcracks' formation and evolution mechanisms are presented and critically analyzed. Secondly, recent advancements in mitigation strategies to prevent degradation in Ni–rich NCM/NCA are highlighted. These strategies include doping, surface coating, structural optimization, and morphology engineering. Finally, we provide an outlook and perspective to identify promising strategies that may enable the practical application of Ni–rich NCM/NCA in commercial settings.

1. Introduction

Lithium-ion batteries (LIBs) are critical in powering electric vehicles (EVs) to reduce CO2 emissions and replace internal combustion engines.[1] The evolution of EVs demands LIBs with higher energy and power densities, extended calendar life, enhanced safety, and affordability. Ni–rich Layered $LiNi_xCo_yMn(Al)_{1-x-y}O_2$ (NCM(A)) materials, with their high capacity, cost–effectiveness, and safety, are promising cathodes for high–energy LIBs.[2]

As shown in Figure 1a–b, when increasing the Ni content in ternary layered cathodes, the reversible specific capacity increases with a given cut–off voltage. However, the structural stability is decreased due to crack formation, deriving from the volume's shrinkage/expansion of the unit cell of NCM/NCA or due to the propagation of surface side reactions.[3] Especially when the Ni content exceeds 80% in the layered ternary cathode,[4] the mechanical stress resulting from the drastic changes of lattice parameters and surface degradation at high

voltage operation induces severe microcracks generation (Figure 1c). The formation of microcracks exposes new internal surfaces within the particles, thereby further accelerating the degradation of cathode/electrolyte interface and bulk structure.[5] Even low–Ni NCM cathodes can undergo structural collapse at high states of charge (SOC) due to substantial unit cell shrinkage.[6] At high SOC, Ni–rich layered cathodes release singlet oxygen [O], which leads to surface degradation and forms rock–salt type NiO impurities on the particle surface, ultimately hampering the Li^+ transport and thus causing loss of active material and overpotential.[2g] Upon consecutive exposure to new particle surfaces through cracking, this process repeats, leading to cycling decay and potential hazards due to the massive cathode/electrolyte side reaction.[7] Therefore, it is critical to stabilize Ni–rich NCM/NCA cathodes by strengthening the bulk structure and suppressing the cathode/electrolyte interphase at high SOC.

This work comprehensively analyzes and summarizes the formation of microcracks and their structural implications in Ni-rich layered cathodes. The generation mechanisms of intergranular cracks are examined from a chemical and mechanical viewpoint, and the corresponding mitigation strategies, including elemental doping strategies, surface coating techniques, concentration gradient design, and single crystal structure optimization, are presented and compared. Finally, a perspective on future directions in Ni–rich cathode design is given.

2. The Mechanism of Microcrack Formation

A comprehensive understanding of the phase transformations occurring during cyclic charge/discharge of Ni–rich NCM/NCA is critical for mechanistic studies. Ni–rich cathode materials suffer from mechanical stress and strain inside the particles between primary particles induced by its anisotropic volume changes, which has been linked with intergranular fracture formation

[a] T. Xu, J. Wu, Dr. J. Ding, Y. Huang
State Key Laboratory of Chemistry and Utilization of Carbon-Based Energy Resources; College of Chemistry, Xinjiang University, Urumqi, 830017, Xinjiang, PR China
E-mail: dingjuan@xju.edu.cn

[b] Dr. W. Zhao
Institute of Nanotechnology, Karlsruhe Institute of Technology (KIT), Herrmann-von-Helmholtz-Platz 1, 76344 Eggenstein-Leopoldshafen, Germany
E-mail: wengao.zhao@kit.edu

[c] Y. Huang
School of Metallurgy and Environment, Central South University, Changsha, 410083
E-mail: yingdecsu@foxmail.com

ChemElectroChem

Review
doi.org/10.1002/celc.202300802

Chemistry Europe
European Chemical
Societies Publishing

and after repetitive charge/discharge, particle pulverization,[11] which leads to massive parasitic reaction products along the forming microcracks. Based on the in–situ X-ray diffraction (XRD) patterns of NCM622 and NCM811, Zheng. et al. claim that the phase transition process may be influenced by the transition metal (TM) or lithium (Li) environments, further confirmed by ex–situ solid–state Nuclear Magnetic Resonance (ss-NMR) spectroscopy shown in Figure 2a.[12] The ^6Li spin–echo *ex-situ* ss-NMR spectra of NCM811 during the first cycle exhibit similar peak shift trends observed in NCM622. Notably, a significant peak shift between $Li_{0.91}$ and $Li_{0.80}$ indicates the extraction of Li_M at this stage. At the same time, the simultaneous appearance of the H2 phase provides further evidence for its association with Li_M deintercalation. The ss-NMR spectral analysis at higher SOC reveals that the Li–ion fully migrates away from the Li_{Ni} site upon (H3-1 phase) formation, which coincides with lattice parameter c reduction. When charging from $Li_{0.80}$ to $Li_{0.34}$, the primary resonance gradually shifts to a lower frequency, in line with the loss of paramagnetic behavior because of the depletion of Jahn–Teller active Ni^{3+}. At the end of charging, an emerging peak is observed around 0 ppm, which the authors assign to the rearrangement of Li^+ near the Ni site (Li_{Ni}).

Yang et al. investigated the transformation mechanism between H1/H2/H3 phase transitions of NCM811, as depicted schematically in Figure 2b, the pristine structure is referred to as H1. Upon charging, Li_M is gradually extracted from the material, resulting in the formation of the H2 phase. The H3 phase can be further divided into two distinct parts (marked as H3-1 and H3-2). The Li-ions in H3-1 tend to escape from the Li_M site, whereas the Li–ion may undergo reordering to form Li-reordered material in H3-2. Therefore, the H1/H2/H3 phase transition can be analyzed from the perspective of the Li–ion environment in the NCM, offering an effective approach to address structural decay caused by microcracks.

Ryu et al. investigated the capacity decay mechanism of Ni–rich ternary layered cathode materials through testing a series of $LiNi_xCo_yMn_{1-x-y}O_2$ (x=0.6, 0.8, 0.9, 0.95, 1).[10] The NCMs display an increased capacity with the increase of Ni content at 4.3 V (vs. Li^+/Li) cutoff voltage operation, in line with findings by other researchers, while the cycling stability is compromised.[13] To explore the phase transition process, the authors employed *in-situ* XRD to track the NCM's crystal structure variation at the first charge cycling (Figure 2c). The diffraction peak position of (003) primarily corresponded to alterations in crystalline cell dimensions along the c-axis direction. The (003) diffraction peak shift to smaller degree indicates an initial expansion of the unit cell of NCM along the c-axis direction, followed by subsequent contraction. Moreover, with the increase of Ni content in the NCM cathode, there is a noticeable increase in the extent of contraction along c-axis. The NCM622 exhibits a shrinkage of only 2.6% along the c-axis

Tianmei Xu is an M.S. candidate majoring in Chemistry at Xinjiang University. She received her B.S. degree in Chemistry from Baoji University of Arts and Sciences in 2023. Her research focuses on the modification of cathode materials to improve their comprehensive performance in lithium–ion batteries under the supervision of Associate Professor Juan Ding.
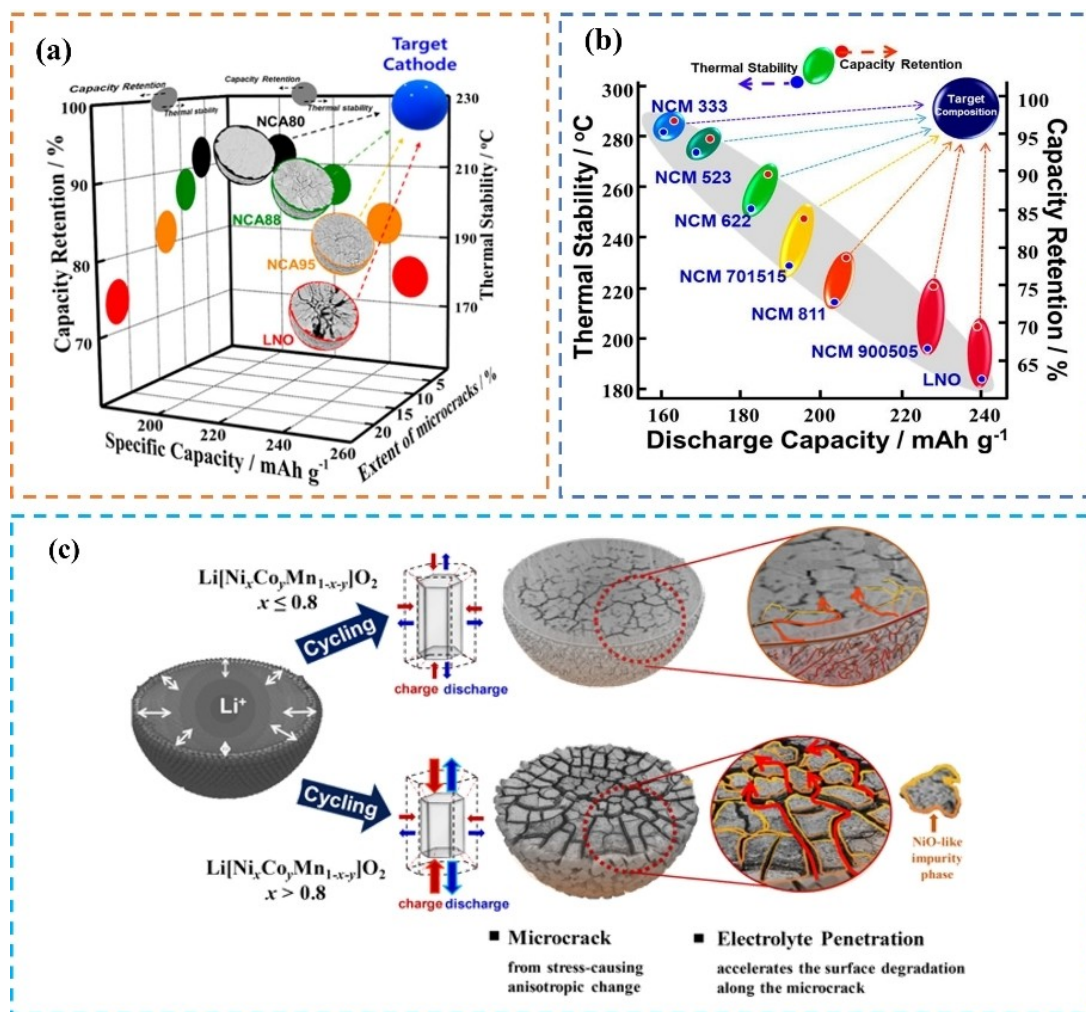
Juan Ding received her Ph. D degree in 2022 from the College of Chemistry, Xinjiang University. She is currently working at Xinjiang University as an associate professor. Her research interests include the manufacture of nanostructured electrodes and their applications for energy conversion and storage.

Ying-de Huang obtained his master's degree from Central South University in 2020. He is currently a Ph.D. candidate in the School of Metallurgy and Environment at Central South University. His current research interest is electrochemical energy storage systems.

Dr. Wengao Zhao is a senior researcher at Karlsruhe Institute of Technology (KIT), Germany. He received Ph. D degree in 2018 from Xiamen University. He studied at Pacific Northwest National Laboratory (USA) from 2016 to 2018 as a joint Ph. D student and worked at the Swiss Federal Laboratory of Materials Science and Technology from 2020 to 2022 as a postdoctoral researcher. His research focuses on exploring the degradation mechanism of advanced cathode materials (e.g. layered Ni–rich NCM) in non–aqueous conventional and solid-state Lithium-ion batteries. He has published more than 60 papers in peer–reviewed journals with a citation more than 6000 times (Google Scholar).

ChemElectroChem

Review
doi.org/10.1002/celc.202300802

Chemistry
Europe
European Chemical
Societies Publishing

Figure 1. (a) The relationship between Ni content, cracking, and material properties is summarized. Reproduced with permission.[8] Copyright 2019, American Chemical Society. (b) The relationship between discharge capacity, thermal stability, and capacity retention of ternary cathode materials with different nickel contents. Reproduced with permission.[9] Copyright 2019, American Chemical Society. (c) Schematic diagram of NCM microcracks with increased Ni contents and anisotropy. Reproduced with permission.[10] Copyright 2018, American Chemical Society.

direction while it charges to 4.5 V, whereas the Li-$(Ni_{0.95}Co_{0.025}Mn_{0.025})O_2$ demonstrates a shrinkage of 6.9% in same direction due to more Li^+ extracted. The repetitive anisotropic expansion and contraction during the charging and discharging process results in intergranular cracks due to induced internal stresses.

Gyeong Won Nam et al. thoroughly compared the particle internal structure's evolution at the different charge/discharge states of NCA by combining advanced characterization techniques.[8] As displayed in Figure 2d, crack initiation was observed from the core of the secondary particle structure. When $Li_xNi_{0.8}Co_{0.15}Al_{0.05}O_2$ is charged to a cut–off voltage of 4.3 V, its cracked area reaches about 7.5% of the total cross–section. It is worth noting that the crack formation is irreversible and that cracks formed during the charge do not close upon expansion of the material during discharge. Interestingly, these cracks cause more damage to the interior of the secondary particle structure than the particle surface. Therefore, it is highly

valuable to develop strategies to impede the formation of microcracks in accordance with their underlying mechanisms.

3. Chemical Modification Strategies

Researchers have been exploring diverse enhancement strategies to solve the challenges associated with Ni–rich NCM/NCA. The approaches were employed to tackle these issues and improve the electrochemical performance of Ni–rich NCM/NCA primarily encompass elemental doping, surface coating, concentration gradient design, and single–crystal structure.[14] Foreign elemental doping (Al, Ti, Zr, et al.) can be an effective strategy to obtain improved material by replacing atoms in the lattice, e.g., by reducing the Li^+/Ni^{2+} cation disorder in Ni–rich NCM or improving their structural stability.[15] The cycling performance and structural stability of $Li[Ni_{0.90}Co_{0.05}Mn_{0.05}]O_2$ (NCM90) cathode is significantly enhanced by introducing Boron (B) dopant.[16] Density functional theory analysis demon-
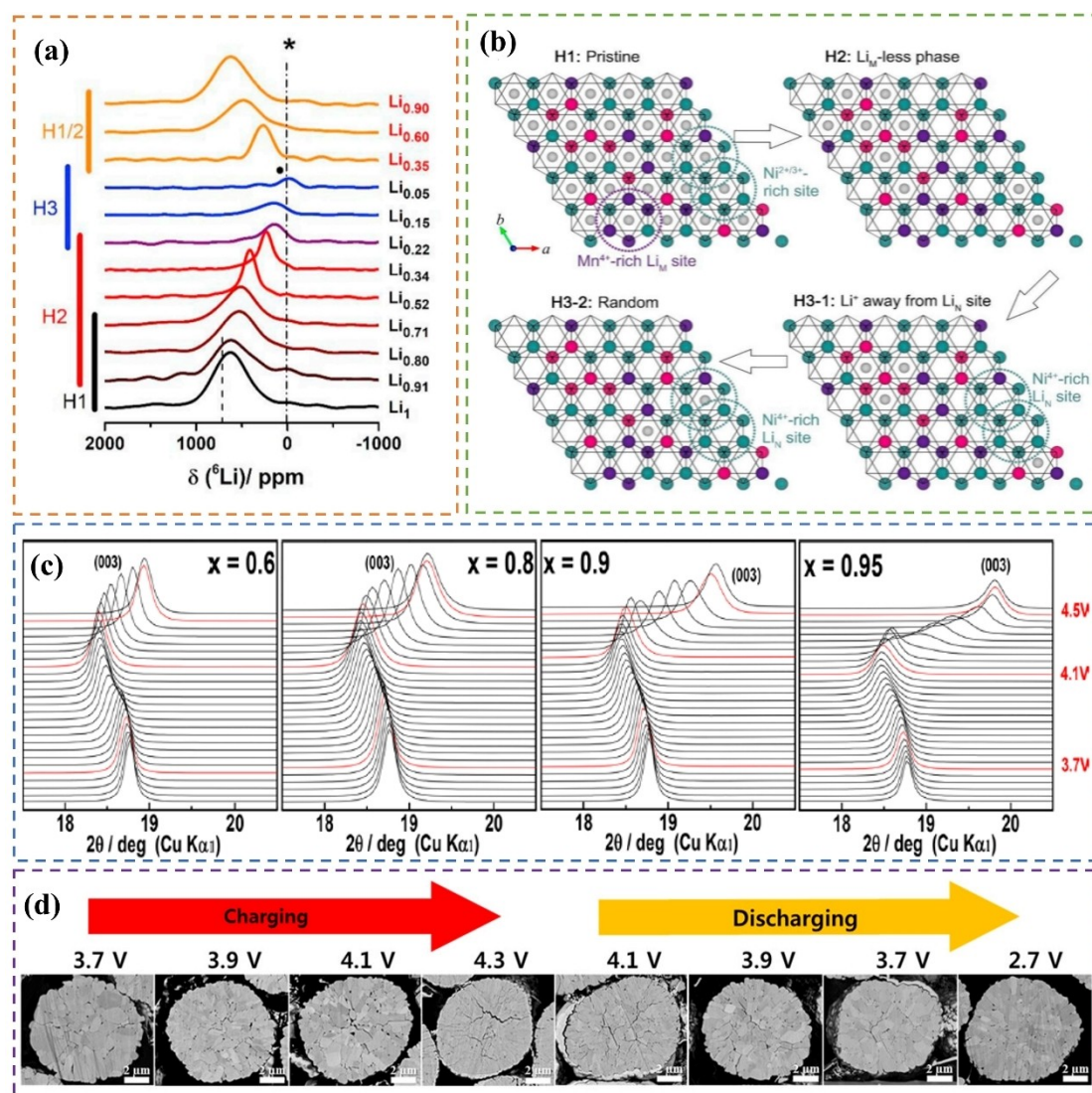
Figure 2. (a) Li spin–echo ex-situ NMR spectrum of the first cycle of NCM811 and (b) Schematic diagram of the local environment of Li-ion in relation to the phase transition. Reproduced with permission.[12] Copyright 2019, Elsevier. (c). (003) reflection of $LiNi_xCo_yMn_{1-x-y}O_2$ (x = 0.6, 0.8, 0.9, and 0.95) during the first cycle charge. Reproduced with permission.[10] Copyright 2018, American Chemical Society. (d) Cross–sectional Scanning Electron Microscope (SEM) image of $Li_xNi_{0.8}Co_{0.15}Al_{0.05}O_2$ positive electrode during charging and discharging process. Reproduced with permission.[8] Copyright 2019, American Chemical Society.

strated that introducing 1 mol% B dopant alters the surface energy and induces a highly textured microstructure, effectively mitigating the internal strain generated during the high SOC of NCM90 cathode. The enhanced structural robustness is attributed to the formation of an arranged rod–like microstructure (primary particles) inside the B-doped NCM90 secondary particle, substantially improving the cyclability by aligning the anisotropic lattice variation to allow single grains to "breathe" without inducing secondary particle fracture. Meanwhile, co-doping cations and anions is also a fashionable strategy, which aims to simultaneously replace TM/Li and oxygen positions in Ni–rich NCM/NCA cathodes.[17] However, the exploration of the intricate interaction mechanisms between different elements is still insufficient, and further fundamental studies assessing the role of single modification, such as sole modification of oxygen

or transition metal sites, respectively, are likely more conducive to advancing the design of more stable cathodes.

Surface coating is another promising strategy to maintain a stable material by inhibiting or weakening detrimental side reactions between the cathode and electrolyte.[2f,18] The ideal coating layer should not only prevent the cathode's surface from electrolyte corrosion but also guarantee smooth Li-ion transport and electronic contact. Currently, a variety of surface modification methods have been developed, including mechanical mixing, sol–gel, pulsed layer deposition (PLD), chemical vapor deposition (CVD), and atomic layer deposition (ALD).[19] Transition metal oxides are typical coating materials that are widely used to maintain surface stability in Ni–rich NCM cathodes, such as Al_2O_3,[20] SiO_2,[21] TiO_2,[22] CeO_2[23] and ZrO_2.[24] Fluorides, such as LiF,[25] AlF_3,[26] and CaF_2[27] are another class of materials utilized for surface modification of cathode materials

as they mitigate cathode/electrolyte interfacial side reactions and transition metal dissolution. Moreover, fluoride salts reduce the charge–transfer resistance. They are able to maintain a benign Li–ion conductivity of the modified particle surface, resulting in an enhanced long–term cyclability and rate capability of the Ni–rich NCM/NCA cathode, even at high temperatures.[28]

Yu. et al. proposed that designing a certain concentration gradient structure is one of the effective strategies to improve the structural stability of Ni–rich ternary layered NCM/NCA.[29] The concept of concentration gradient structure was originally derived from the core–shell structure. It can be separated into the following strategies: shell concentration gradient, full concentration gradient, and double inclined concentration gradient.[30] The basic concept of the concentration gradient is to utilize less stable but high capacity Ni–rich NCM as the inner component and the more stable but lower capacity low–Ni NCM as the outer component. This structure aims to strike an optimal balance between cycling stability and high capacity by synthesizing an extremely durable but still decent capacity outer component, which is stable enough to prevent exposure of the labile core upon repeated cycling. The outer layer is typical Mn–rich NCM, which effectively minimizes undesired

side reactions between the active cathode and electrolyte, while the Ni–rich NCM allows for high capacity at moderate cut–off voltage.

Amine et al. investigated a concentration–gradient layered NCM cathode,[31] as illustrated in Figure 3c, with an average composition of $Li[Ni_{0.64}Co_{0.18}Mn_{0.18}]O_2$ (NCM64). The material gradually decreases the Ni concentration from the core to the surface region. For example, the NCM64 with a concentration gradient exhibits a comparable capacity (209 mAh g^{-1} vs 212 mAh g^{-1}) to the conventional NCM811. The surface layer of the concentration–gradient material consists of Mn^{4+}-rich Li-$[Ni_{0.46}Co_{0.23}Mn_{0.31}]$ O$_2$ with lower nickel content, the lower content of Ni^{4+} formed, caused in part by substitution of Nickel and in part by the suppression of the average nickel oxidation due to Mn inclusion, compared to that of $Li[Ni_{0.8}Co_{0.1}Mn_{0.1}]$ O$_2$ at high SOC, thus suppressing the decomposition of electrolyte and gain better cycling stability. Notably, the onset of the H3 phase transformation of low–Ni NCM at the outer layer is relatively retarded, while the high–Ni NCM exhibits a sudden lattice contraction during the formation of the H3 phase, thus preventing the propagation of microcrack to the outer layer deriving from the inner of the particles. The Ni–rich NCM64 cathode with concentration gradient structure significantly
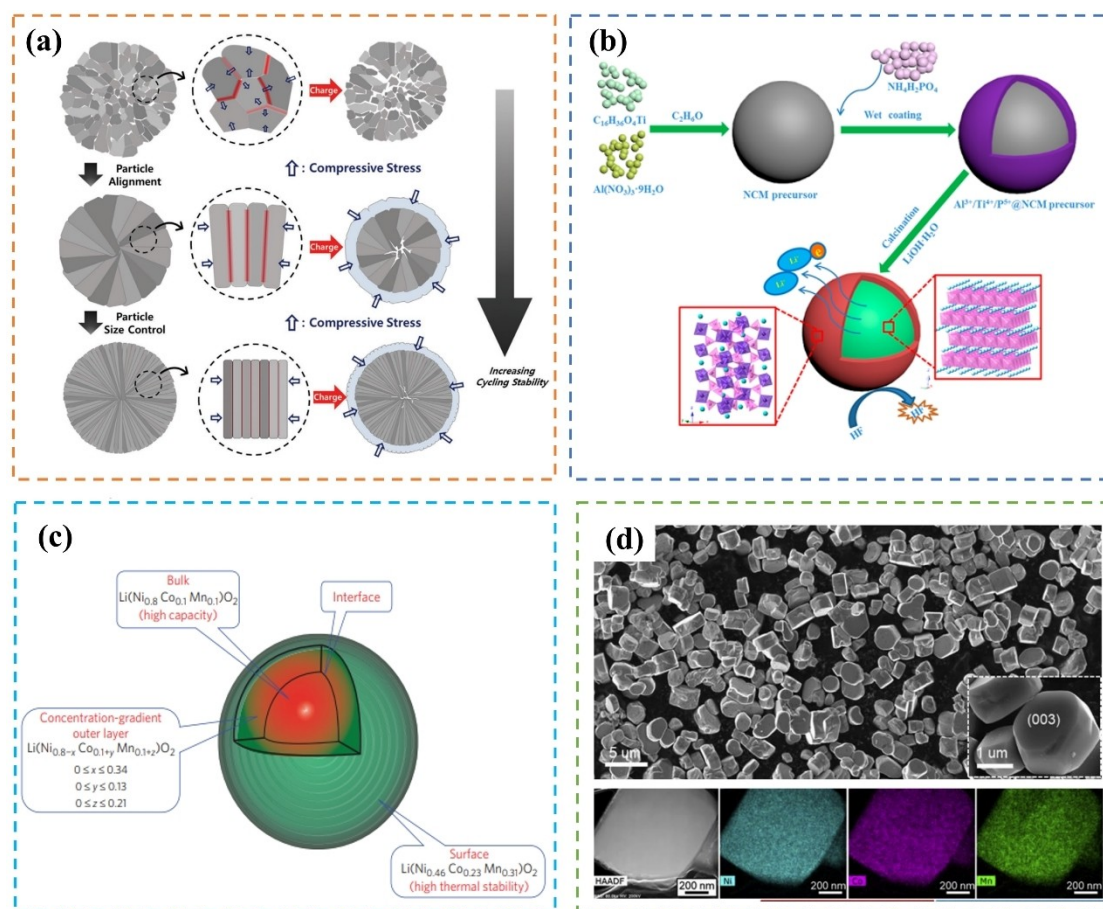
Figure 3. High–Ni NCM/NCA cathode modification method to address the crack formation: (a) ion doping. Reproduced with permission.[16] Copyright 2020, Wiley-VCH; (b) surface coating. Reproduced with permission.[38] Copyright 2019, American Chemical Society; (c) concentration gradient. Reproduced with permission.[31] Copyright 2009, Springer Nature; (d) Monocrystalline structure strategy. Reproduced with permission.[37] Copyright 2020, Elsevier.

ChemElectroChem

Review

doi.org/10.1002/celc.202300802

**Chemistry
Europe**

European Chemical
Societies Publishing

enhances the stability of bulk structure and cathode/electrolyte interphase while maintaining a comparable capacity and superior cycling stability to conventional NCM811.

Beyond doping and coating, modulating the microstructure of Ni–rich NCM/NCA cathodes has also been proven to be an effective strategy for improving their comprehensive performance.[14a] The conventional NCM/NCA exists as secondary particles, composed of numerous primary particles, typically dubbed a polycrystalline morphology. As outlined above, polycrystalline NCM suffers from severe intergranular cracking along grain boundaries due to anisotropic contraction and expansion of primary particles and potentially surface side reactions, thereby exposing the interior of the particles to the electrolyte and consecutively pulverizing the cathode active material (CAM) particles.[32] In the absence of grain boundary, the single–crystalline (SC) primary particles with a diameter of 2–4 μm can by definition not undergo intergranular cracking and thus are a promising strategy to alleviate the formation of micro/nano–cracks and the associated degradation.[33] Moreover, the unique SC structure is also beneficial to alleviate the accumulation of side reaction products and unexpected phase transformation due to the limited electrode/electrolyte interphase area.[34] Therefore, the Ni–rich SC-NCM primary particles offer a promising strategy to strengthen the structural stability and suppress the interphase parasitic reactions, achieving enhanced cycling performance and thermal stability.[35] Dahn et al. investigated the electrochemical properties of polycrystalline and single–crystal $Li[Ni_{0.5}Co_{0.2}Mn_{0.3}]O_2$ (NCM523) using X-ray diffraction.[36] The results showed that the lattice parameter evolution is consistent for both materials. However, the single–crystal NCM523 maintains a more robust bulk structure due to the irrelevance of anisotropic volume change if the CAM consists of isolated grains. The stress evolution was simulated in a cylindrical model, revealing that axial and tangential stresses were concentrated on the single–crystal surface during charging, just resulting in slight microcrack formation along the (003) crystal surface of SC-NCM622, which does not significantly draw from the cycling stability under high–voltage operation (Figure 3d).[37]

In summary, the four presented strategies, chemical modification, surface coating, concentration gradient, and single crystal structure, have all been shown to be beneficial to enhancing electrochemical performance and thermal stability by stabilizing the cathode/electrolyte interphase and/or bulk structure of NCM and NCA cathodes. However, these strategies are still not perfect, and further research on the properties of layered NCM and NCA materials is necessary to facilitate their wide application in various industries. Specifically, chemical modification typically reduces the capacity and increases costs due to additional steps and the use of expensive materials, whereas surface coating is an additional step and does not help if the electrolyte penetrates inside the particle. Moreover, concentration transient limits the overall achievable capacity and requires the simultaneous synthesis of multiple phases, which means that the optimal calcination temperature for most of the phases must be sub–optimal, while the single–crystalline particles are stable, but the rate capability is necessary to be improved.

4. Conclusion and Perspectives

This mini–review thoroughly examines and contrasts the four primary strategies to address crack formation in Ni–rich NCM/ NCA cathodes. Conventional NCM/NCA cathodes deliver enhanced capacity when the Ni content is increased. Still, cycling retention and thermal stability properties are decreased due to the higher SOC reached at comparable cut–off voltages. This results in a propensity for crack formation within the bulk structure and oxygen release at the particle surface. Individual strategies typically target specific issues, such as surface or bulk structural stability. However, these isolated approaches often fail to address all the challenges associated with Ni–rich materials. Consequently, a synergistic approach, combining multiple modifications, emerges as a promising strategy. Therefore, combining multiple modifications would be a promising strategy to improve the stability of the cathode/electrolyte interphase, bulk structure, and even thermal stability due to their combined effects. The developed strategies must be scalable for practical application, especially in commercial production. Therefore, only those modifications that utilize readily available materials and scalable processing steps should be considered.

Author Contributions

Tianmei Xu: Investigation, Methodology, Visualization, Writing– original draft. Jingjing Wu: Writing–review & editing. Juan Ding: Validation, Writing–review & editing. Yingde Huang: Software, Validation, Writing–review & editing. Yudai Huang: Resources, Funding acquisition, Project administration,. Wengao Zhao: Conceptualization, Supervision, Writing–review & editing.

Acknowledgements

Conflict of Interests

There are no conflicts to declare.

Data Availability Statement

The data that support the findings of this study are available from the corresponding author upon reasonable request.

[1] a) M. Jiang, D. L. Danilov, R.-A. Eichel, P. H. L. Notten, *Adv. Energy Mater.* **2021**, *11*, 2103005; b) L. Liang, X. Li, F. Zhao, J. Zhang, Y. Liu, L. Hou, C. Yuan, *Adv. Energy Mater.* **2021**, *11*, 2170079.
[2] a) W.-J. Zhang, *J. Power Sources* **2011**, *196*, 2962; b) R. Yazami, N. Lebrun, M. Bonneau, M. Molteni, *J. Power Sources* **1995**, *54*, 389; c) X. Zhu, F. Meng, Q. Zhang, L. Xue, H. Zhu, S. Lan, Q. Liu, J. Zhao, Y. Zhuang, Q. Guo, B. Liu, L. Gu, X. Lu, Y. Ren, H. Xia, *Nat. Sustainability* **2021**, *4*, 392; d) J. Kim, H. Lee, H. Cha, M. Yoon, M. Park, J. Cho, *Adv. Energy Mater.* **2018**, *8*, 1702028; e) Z. Tan, X. Chen, Y. Li, X. Xi, S. Hao, X. Li, X. Shen, Z. He, W. Zhao, Y. Yang, *Adv. Funct. Mater.* **2023**, *33*, 2215123; f) Z. Tan, Y. Li, X. Xi, S. Jiang, X. Li, X. Shen, Z. He, *ACS Appl. Mater. Interfaces* **2023**, *15*, 8555; g) Z. Tan, Y. Li, X. Xi, S. Jiang, X. Li, X. Shen, P. Zhang, Z. He, *Nano Res.* **2023**, *16*, 4950; h) L. Ni, H. Chen, W. Deng, B. Wang, J. Chen, Y. Mei, G. Zou, H. Hou, R. Guo, J. Xie, X. Ji, *Adv. Energy Mater.* **2022**, *12*, 2103757; i) L. Ni, H. Chen, S. Guo, A. Dai, J. Gao, L. Yu, Y. Mei, H. Wang, Z. Long, J. Wen, W. Deng, G. Zou, H. Hou, T. Liu, K. Amine, X. Ji, *Adv. Funct. Mater.* **2023**, *33*, 2307126; j) L. Ni, H. Chen, J. Gao, Y. Mei, H. Wang, W. Deng, G. Zou, H. Hou, X. Ji, *ACS Nano* **2023**, *17*, 12759; k) L. Ni, H. Chen, J. Gao, Y. Mei, H. Wang, F. Zhu, J. Huang, B. Zhang, W. Xu, B. Song, Y. Zhang, W. Deng, G. Zou, H. Hou, Y. Zhou, X. Ji, *Nano Energy* **2023**, *115*, 108743.
[3] a) S. S. Zhang, *Energy Storage Mater.* **2020**, *24*, 247; b) S. Lee, L. Su, A. Mesnier, Z. Cui, A. Manthiram, *Joule* **2023**, *7*, 2430.
[4] a) Y. Su, Q. Zhang, L. Chen, L. Bao, Y. Lu, S. Chen, F. Wu, *J. Energy Chem.* **2022**, *65*, 236; b) W. Xue, M. Huang, Y. Li, Y. G. Zhu, R. Gao, X. Xiao, W. Zhang, S. Li, G. Xu, Y. Yu, P. Li, J. Lopez, D. Yu, Y. Dong, W. Fan, Z. Shi, R. Xiong, C.-J. Sun, I. Hwang, W.-K. Lee, Y. Shao-Horn, J. A. Johnson, J. Li, *Nat. Energy* **2021**, *6*, 495.
[5] a) S. Yin, W. Deng, J. Chen, X. Gao, G. Zou, H. Hou, X. Ji, *Nano Energy* **2021**, *83*, 105854; b) L. Liang, X. Li, M. Su, L. Wang, J. Sun, Y. Liu, L. Hou, C. Yuan, *Angew. Chem. Int. Ed.* **2023**, *62*, e202216155.
[6] W. Li, H. Y. Asl, Q. Xie, A. Manthiram, *J. Am. Chem. Soc.* **2019**, *141*, 5097.
[7] a) Z. Tan, Y. Li, X. Xi, S. Jiang, X. Li, X. Shen, P. Zhang, Z. He, J. Zheng, *J. Energy Chem.* **2022**, *72*, 570; b) Z. Tan, Y. Li, X. Xi, S. Jiang, X. Li, X. Shen, S. Hao, J. Zheng, Z. He, *ACS Sustainable Chem. Eng.* **2022**, *10*, 3532; c) J. Zhang, H. He, X. Wang, G. Mao, W. Yu, Z. Ding, Q. Tian, H. Tong, X. Guo, *Appl. Surf. Sci.* **2022**, *589*, 152878; d) J. Liu, W. Jiao, X. Wang, G. Mao, Y. Yao, W. Yu, H. Tong, *Ceram. Int.* **2023**, *49*, 13953; e) Y. Huang, P.-Y. Li, H.-X. Wei, Y.-H. Luo, L.-B. Tang, H.-Z. Chen, X.-H. Zhang, J.-C. Zheng, *Chem. Eng. J.* **2023**, *477*, 146850.
[8] G. W. Nam, N.-Y. Park, K.-J. Park, J. Yang, J. Liu, C. S. Yoon, Y.-K. Sun, *ACS Energy Lett.* **2019**, *4*, 2995.
[9] Y.-K. Sun, *ACS Energy Lett.* **2019**, *4*, 1042.
[10] H.-H. Ryu, K.-J. Park, C. S. Yoon, Y.-K. Sun, *Chem. Mater.* **2018**, *30*, 1155.
[11] H. Yang, H.-H. Wu, M. Ge, L. Li, Y. Yuan, Q. Yao, J. Chen, L. Xia, J. Zheng, Z. Chen, J. Duan, K. Kisslinger, X. C. Zeng, W.-K. Lee, Q. Zhang, J. Lu, *Adv. Funct. Mater.* **2019**, *29*, 1808825.
[12] S. Zheng, C. Hong, X. Guan, X. Xiang, X. Liu, G.-L. Xu, R. Liu, G. Zhong, F. Zheng, Y. Li, X. Zhang, Y. Ren, Z. Chen, K. Amine, Y. Yang, *J. Power Sources* **2019**, *412*, 336.
[13] L. de Biasi, A. O. Kondrakov, H. Geßwein, T. Brezesinski, P. Hartmann, J. Janek, *J. Phys. Chem. C* **2017**, *121*, 26163.
[14] a) L. Ni, S. Zhang, A. Di, W. Deng, G. Zou, H. Hou, X. Ji, *Adv. Energy Mater.* **2022**, *12*, 2201510; b) W. Huang, W. Li, L. Wang, H. Zhu, M. Gao, H. Zhao, J. Zhao, X. Shen, X. Wang, Z. Wang, C. Qi, W. Xiao, L. Yao, J. Wang, W. Zhuang, X. Sun, *Small* **2021**, *17*, 2104282; c) U.-H. Kim, J.-H. Park, A. Aishova, R. M. Ribas, R. S. Monteiro, K. J. Griffith, C. S. Yoon, Y.-K. Sun, *Adv. Energy Mater.* **2021**, *11*, 2100884.
[15] a) C.-H. Jung, D.-H. Kim, D. Eum, K.-H. Kim, J. Choi, J. Lee, H.-H. Kim, K. Kang, S.-H. Hong, *Adv. Funct. Mater.* **2021**, *31*, 2010095; b) D. Kong, J. Hu, Z. Chen, K. Song, C. Li, M. Weng, M. Li, R. Wang, T. Liu, J. Liu, M. Zhang, Y. Xiao, F. Pan, *Adv. Energy Mater.* **2019**, *9*, 1901756; c) F. Schipper, H. Bouzaglo, M. Dixit, E. M. Erickson, T. Weigel, M. Talianker, J. Grinblat, L. Burstein, M. Schmidt, J. Lampert, C. Erk, B. Markovsky, D. T. Major, D. Aurbach, *Adv. Energy Mater.* **2018**, *8*, 1701682; d) W. Zhao, L. Zou, H. Jia, J. Zheng, D. Wang, J. Song, C. Hong, R. Liu, W. Xu, Y. Yang, J. Xiao, C. Wang, J.-G. Zhang, *Appl. Energy Mater.* **2020**, *3*, 3369.
[16] H.-H. Ryu, N.-Y. Park, D. R. Yoon, U.-H. Kim, C. S. Yoon, Y.-K. Sun, *Adv. Energy Mater.* **2020**, *10*, 2000495.
[17] L. Qiu, W. Xiang, W. Tian, C.-L. Xu, Y.-C. Li, Z.-G. Wu, T.-R. Chen, K. Jia, D. Wang, F.-R. He, X.-D. Guo, *Nano Energy* **2019**, *63*, 103818.
[18] D. Becker, M. Börner, R. Nölle, M. Diehl, S. Klein, U. Rodehorst, R. Schmuch, M. Winter, T. Placke, *ACS Appl. Mater. Interfaces* **2019**, *11*, 18404.
[19] X. Tan, M. Zhang, J. Li, D. Zhang, Y. Yan, Z. Li, *Ceram. Int.* **2020**, *46*, 21888.
[20] R. S. Negi, E. Celik, R. Pan, R. Stäglich, J. Senker, M. T. Elm, *ACS Appl. Energ. Mater.* **2021**, *4*, 3369.
[21] W. Cho, S.-M. Kim, J. H. Song, T. Yim, S.-G. Woo, K.-W. Lee, J.-S. Kim, Y.-J. Kim, *J. Power Sources* **2015**, *282*, 45.
[22] Q. Fan, K. Lin, S. Yang, S. Guan, J. Chen, S. Feng, J. Liu, L. Liu, J. Li, Z. Shi, *J. Power Sources* **2020**, *477*, 228745.
[23] H. Yu, H. Zhu, H. Jiang, X. Su, Y. Hu, H. Jiang, C. Li, *Natl. Sci. Rev.* **2023**, *10*, nwac166.
[24] L. Yao, F. Liang, J. Jin, B. V. R. Chowdari, J. Yang, Z. Wen, *Chem. Eng. J.* **2020**, *389*, 124403.
[25] J. Huang, K. Du, Z. Peng, Y. Cao, Z. Xue, J. Duan, F. Wang, Y. Liu, G. Hu, *ChemElectroChem* **2019**, *6*, 5428.
[26] G. Hu, X. Qi, K. Hu, X. Lai, X. Zhang, K. Du, Z. Peng, Y. Cao, *Electrochim. Acta* **2018**, *265*, 391.
[27] S. Dai, G. Yan, L. Wang, L. Luo, Y. Li, Y. Yang, H. Liu, Y. Liu, M. Yuan, *J. Electroanal. Chem.* **2019**, *847*, 113197.
[28] B.-C. Park, H.-B. Kim, H. J. Bang, J. Prakash, Y.-K. Sun, *Ind. Eng. Chem. Res.* **2008**, *47*, 3876.
[29] K. Wu, J. Wang, Q. Li, Y. Yang, X. Deng, R. Dang, M. Wu, Z. Wu, X. Xiao, X. Yu, *Nanoscale* **2020**, *12*, 11182.
[30] a) J.-Y. Liao, A. Manthiram, *J. Power Sources* **2015**, *282*, 429; b) C. Zhang, T. Li, B. Xue, X. Wu, L. Li, Y. Guo, L. Zhang, *Chem. Eng. J.* **2023**, *451*, 138518.
[31] Y.-K. Sun, S.-T. Myung, B.-C. Park, J. Prakash, I. Belharouak, K. Amine, *Nat. Mater.* **2009**, *8*, 320.
[32] L. Ni, R. Guo, W. Deng, B. Wang, J. Chen, Y. Mei, J. Gao, X. Gao, S. Yin, H. Liu, S. Zhang, G. Zou, H. Hou, X. Ji, *Chem. Eng. J.* **2022**, *431*, 133731.
[33] Y.-G. Zou, H. Mao, X.-H. Meng, Y.-H. Du, H. Sheng, X. Yu, J.-L. Shi, Y.-G. Guo, *Angew. Chem. Int. Ed.* **2021**, *60*, 26535.
[34] a) X. Fan, G. Hu, B. Zhang, X. Ou, J. Zhang, W. Zhao, H. Jia, L. Zou, P. Li, Y. Yang, *Nano Energy* **2020**, *70*, 104450; b) W. Zhao, L. Zou, L. Zhang, X. Fan, H. Zhang, F. Pagani, E. Brack, L. Seidl, X. Ou, K. Egorov, X. Guo, G. Hu, S. Trabesinger, C. Wang, C. Battaglia, *Small* **2022**, *18*, 2107357.
[35] a) X.-M. Fan, Y.-D. Huang, H.-X. Wei, L.-B. Tang, Z.-J. He, C. Yan, J. Mao, K.-H. Dai, J.-C. Zheng, *Adv. Funct. Mater.* **2022**, *32*, 2109421; b) X. Fan, X. Ou, W. Zhao, Y. Liu, B. Zhang, J. Zhang, L. Zou, L. Seidl, Y. Li, G. Hu, C. Battaglia, Y. Yang, *Nat. Commun.* **2021**, *12*, 5320.
[36] R. Weber, C. R. Fell, J. R. Dahn, S. Hy, *J. Electrochem. Soc.* **2017**, *164*, A2992.
[37] G. Qian, Y. Zhang, L. Li, R. Zhang, J. Xu, Z. Cheng, S. Xie, H. Wang, Q. Rao, Y. He, Y. Shen, L. Chen, M. Tang, Z.-F. Ma, *Energy Storage Mater.* **2020**, *27*, 140.
[38] G. Song, H. Zhong, Z. Wang, Y. Dai, X. Zhou, J. Yang, *ACS Appl. Energ. Mater.* **2019**, *2*, 7923.

REVIEW

Microcracks inevitably form in poly-crystalline NCM cathodes during high–voltage operation or prolonged cycling due to internal strain accumulation or phase transition. To address this issue, single or multiple modification strategies such as elemental doping, building single–crystal structures, surface coating, and concentration gradient design can help mitigate microcrack formation and improve cycling capability.
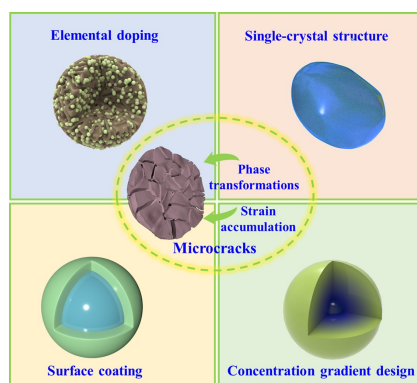
T. Xu, J. Wu, Dr. J. Ding*, Y. Huang*, Y. Huang, Dr. W. Zhao*

1 – 8

Advancements in Addressing Microcrack Formation in Ni–Rich Layered Oxide Cathodes for Lithium–Ion Batteries